IOP Conference Series: Materials Science and Engineering

PAPER • OPEN ACCESS

Modified Double Sampling Control Chart for Monitoring The Coefficient of Variation

To cite this article: F Rozi *et al* 2019 *IOP Conf. Ser.: Mater. Sci. Eng.* **598** 012110

IOP Conf. Series: Materials Science and Engineering **598** (2019) 012110 doi:10.1088/1757-899X/598/1/012110

Modified Double Sampling Control Chart for Monitoring The Coefficient of Variation

F Rozi[1], U S Pasaribu[2], U Mukhaiyar[2] and D Irianto[2]

[1]Faculty of Mathematics and Natural Science, Institut Teknologi Bandung, Jl. Ganesha 10 Bandung, Indonesia.
[2]Statistics Research Group FMIPA, Institut Teknologi Bandung, Jl. Ganesha 10 Bandung, Indonesia.
[3]Manufacturing Systems Research Group FTI, Institut Teknologi Bandung, Jl. Ganesha 10 Bandung, Indonesia.

fachrur201@students.itb.ac.id

Abstract. Monitoring the coefficient of variation (CV) has received wide attention in quality control, mainly used when the process mean and standard deviation are not constant. This work proposes a modified Double Sampling (DS) chart for monitoring the CV, denoted DS-*G* chart, in order to improve the sensitivity of previous DS chart for monitoring the CV, denoted DS-γ chart. Some numerical results for statistical properties of the proposed chart and performance comparisons are provided in the form of tables. Based on the average number of observation to signal (ANOS) performance, the proposed DS-*G* chart outperforms the DS-γ chart.

1. Introduction

Quality is the key factors that becomes a strategy to improve productivity in manufacturing or service companies. A control chart as the vital tools in statistical process control (SPC) system is widely used to investigate and determine whether a process is in (statistical) control or not. Under normality distribution, a process is assumed as in-control (IC) during it has a constant mean and standard deviation, but when the mean and/or the standard deviation change, the control chart would trigger an alarm and makes the corresponding process is called to be out-of-control (OC).

Nevertheless, in some conditions, such as biological and chemical assay quality control, the process may not have the constant mean and standard deviation all of time, but if their ratio remains stable around a constant value, the process may be still assumed as IC [1]. In this case, changes of the process variability can be detected by monitoring the coefficient of variation (CV), γ, which is represented as the ratio of the standard deviation σ to the mean μ. There are many opportunities in SPC for monitoring the CV, especially in area of engineering such as manufacturing [2], materials engineering ([3], [4], [5]), and mechanical engineering [6]. Monitoring the process of sintered and cutting tool materials are typical examples from this setting [4].

Kang et al. [7] in 2007, developed the first control chart for monitoring the CV. This chart monitors CV through a Shewhart-type chart (denoted SH-γ chart), making this chart is not sensitive for detecting small-to-moderate CV shifts. Afterward, some extensions are done to enhance the SH-γ chart's sensitivity. Hong et al. [8] proposed the two-sided EWMA-γ chart and Castagliola et al. [9] developed the two one-sided EWMA-γ^2 chart, respectively. Both of charts outperform the SH-γ chart for detecting small-to- moderate CV shifts. The synthetic chart for monitoring the CV (denoted Syn-γ chart) has been investigated by Calzada and Scariano [10]. This chart also performed better than the SH-γ chart.

Furthermore, to enrich the OC detection, some authors have been proposed to implement the adaptive-type control charts, such as variable sampling interval (VSI) and variable sample size (VSS) schemes. Castagliola et al. ([3] and [11]) incorporated the VSI and VSS features in Shewhart type for monitoring the CV (denoted VSI-γ and VSS-γ chart). Their proposed charts show more performs than the SH-γ chart. Furthermore, Amdouni et al. ([12] and [13]) was developed the VSS-γ and VSI-γ chart in short production runs context, respectively. While Khaw et al. [14] investigated the combine of The VSS and VSI for monitoring the CV (denoted VSSI-γ chart).

The Double Sampling (DS) chart uses the both ideas of VSI and VSS. In case an OC warning or signal occurs, in addition to the first sample, the second sample is observed with zero (the shortest) time intervals. The first DS chart was proposed by Croasdale [15] for monitoring the mean process (denoted DS-$\bar{X}$ chart). This chart evaluated the information from the first and second samples independently. Furthermore, Daudin [16] modified the DS-$\bar{X}$ chart of Croasdale [15] that utilizes the information from both samples at the second sample stage. Irianto and Shinozaki [17] discussed both DS procedures and stated that the Daudin's DS chart has a higher capability than to Croasdale's DS chart for shift detection.

Concerning the CV chart, in the recent works on the DS-type chart, Ng et al. [18] applied the DS approach into the CV chart (denoted DS-γ chart) and shows this chart's performance significantly surpasses the SH-γ chart in detecting the CV shifts. Note that in DS-γ chart procedure, determining the process conditions at the second sample stage is only used by second sample information. Based on the idea of Daudin [16] which involved both samples information in determining the process condition at second sample stage, the modified the DS-γ chart is proposed, considering the combined information from the first and second samples to draw conclusions in the second sample stage.

The aim of this paper proposes a modified DS procedure for monitoring the CV based on the preliminary work of Ng et al. [18] to improve the performance of DS-γ chart. The remainder of this paper is organized as follows: Section 2 reviews the distribution of sample CV. A brief review of the DS-γ chart and our proposed DS chart for monitoring the CV is presented in Section 3. The statistical properties of the proposed chart are examined in the same section. In Section 4, the numerical analysis and comparison performance of the modified chart are carried out. Finally, the conclusions are drawn in the last section.

Here, we recapitulate some abbreviated expressions used in this paper for easy reference.
DS: Double sampling;
CV: Coefficient of variation;
LWL: Lower warning limit in first stage; UWL: Upper warning limit in first stage;
LCL1: Lower control limit in first stage; UCL1: Upper control limit in first stage;
LCL2: Lower control limit in second stage; UCL2: Upper control limit in second stage;
ANOS: Average number of observation to signal;
IC: in-control; OC: out-of-control;

2. Review of the sample CV distribution

Let X is a positive random variable from the population with mean μ and standard deviation $\sigma < \infty$. Then, the CV of X, notated γ, is defined as

$$\gamma = \frac{\sigma}{\mu} \tag{1}$$

Assume that $\{X_1, X_2, ..., X_m\}$ is random samples of size *m* from a normal $N(\mu, \sigma^2)$ distribution. If $\bar{X}$ and *S* are the sample mean and standard deviation of $\{X_1, X_2, ..., X_m\}$, respectively, i.e.

$$\bar{X} = \frac{1}{m}\sum_{i=1}^{m} X_i \text{ , } S = \left(\frac{\sum_{i=1}^{m}\left(X_i - \bar{X}\right)^2}{m-1} \right)^{1/2} \tag{2}$$

then the sample CV, notated $\hat{\gamma}$, is computed as

$$\hat{\gamma} = \frac{S}{\bar{X}}. \tag{3}$$

Iglewicz et al. [19] showed that the cumulative distribution function (c.d.f.) of $\hat{\gamma}$ can be accurately approximated by the non-central t distribution if $0 < \gamma \leq 0.5.$ Then an approximation for the c.d.f. of $\hat{\gamma}$ is

$$F_{\hat{\gamma}}(x \mid m, \gamma) \approx 1 - F_T\left(\frac{\sqrt{m}}{x} \middle| m-1, \frac{\sqrt{m}}{\gamma} \right) \tag{4}$$

where $F_T(. \mid s, r)$ is the c.d.f. of the non-central *t* distribution with *s* degree of freedom and non-centrality parameter *r*.

3. Modified DS chart for the CV

Suppose that $\{X_{1t}, X_{2t}, ..., X_{nt}\}$ are a subgroups of size *n*, at sample number $t = 1, 2, ...$. If each random variable X_{it}, $i = 1, 2, ..., n$ is assumed independence within and between the subgroups and follows a normal $N(\mu_t, \sigma_t^2)$ distribution, where μ_t and $\sigma_t^{\ 2}$ are expressed as population mean and variance, at sample number *t*, respectively. Here, the IC process in CV is defined as $\gamma_t = \sigma_t / \mu_t = \gamma_0$. This implies that between one subgroup to another, the values of μ_t and σ_t may change, but the CV, $\gamma_t = \sigma_t / \mu_t$ must be remain equal to predefined IC value γ_0, for all the subgroups.

3.1. A brief review of DS-γ chart ([18])

In this subsection, a brief of DS-γ chart proposed by Ng et al. [18] is reviewed. Fig. 1 describes the sampling intervals, where UWL, LWL, UCL_1, LCL_1, UCL_2, and LCL_2, have been mentioned at abbreviated summary in Section 1. It should be noted that $(UWL < UCL_1)$ and $(LCL_1 < LWL)$. The formulas for the control and warning limits of the DS-γ chart are given as

$$\begin{aligned} UWL = \mu_0(\hat{\gamma}) + w\sigma_0(\hat{\gamma});\ \ UCL_1 = \mu_0(\hat{\gamma}) + k_1\sigma_0(\hat{\gamma});\ \ UCL_2 = \mu_0(\hat{\gamma}) + k_2\sigma_0(\hat{\gamma}) \\ LWL = \mu_0(\hat{\gamma}) - w\sigma_0(\hat{\gamma});\ \ LCL_1 = \mu_0(\hat{\gamma}) - k_1\sigma_0(\hat{\gamma});\ \ LCL_2 = \mu_0(\hat{\gamma}) - k_2\sigma_0(\hat{\gamma}) \end{aligned} \tag{5}$$

where $W > 0$ and $L_1 > W$ denote the parameters of the warning and control limits for the first sample stage, respectively, and $L_2 > 0$ denotes the parameter of the control limits for the second sample stage. Here, $\mu_0(\hat{\gamma})$ and $\sigma_0(\hat{\gamma})$ denote the IC-mean and IC-standard deviation of the sample CV, respectively. The formulas of $\mu_0(\hat{\gamma})$ and $\sigma_0(\hat{\gamma})$ can be obtained in detail from [3].

Let define $I_1 = [LWL, UWL]$, $I_2 = (UWL, UCL_1]$, $I_3 = [LCL_1, LWL)$, and $I_4 = (-\infty, LCL_1) \cup (UCL_1, \infty)$. Then according to Fig. 1, the operational procedure of DS-γ chart can be derived as follows:

Step 1. At sample number *t*, take the first sample of size n_1, $X_{1i,t}$, $i = 1, 2, ..., n_1$, from a population that is normally distributed with mean μ_t and variation σ_t^2.

Step 2. Compute the first sample CV, $\hat{\gamma}_{1t} = S_{1t} / \bar{X}_{1t}$. Note that $\bar{X}_{1t}$ and S_{1t} are the sample mean and standard deviation of the first sample which calculate using Eq. (2) with $m = n_1$.

Step 3. If $\hat{\gamma}_{1t} \in I_1$, the process is considered to be IC, and return to Step 1.

Step 4. If $\hat{\gamma}_{1t} \in I_4$, the process is considered to be OC. The control process proceeds to Step 7.

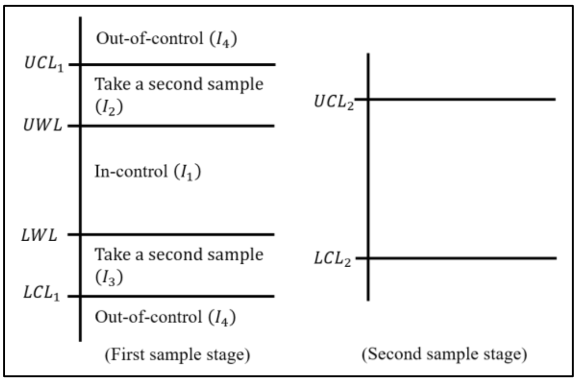

Figure 1. The DS-γ chart procedure [18].

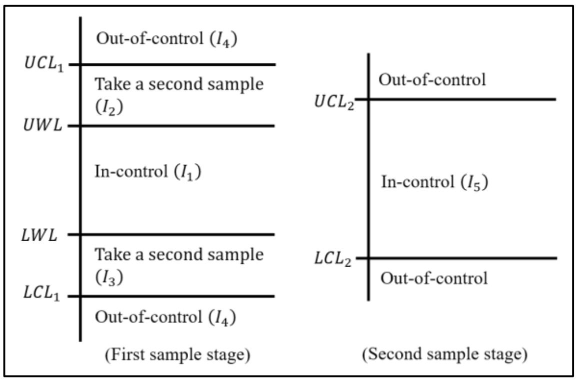

Figure 2. The DS-*G* chart procedure

Step 5. If $\hat{\gamma}_{1t} \in I_2$ or $\hat{\gamma}_{1t} \in I_3$, take the second sample of size n_2, $X_{2i,t}$, $i = 1, 2, ..., n_2$, from the population of the first sample, then compute the second sample CV, $\hat{\gamma}_{2t} = S_{2t} / \bar{X}_{2t}$. Note that $\bar{X}_{2t}$ and S_{2t} are the sample mean and standard deviation of the second sample which obtained by Eq. (2) with $m = n_2$.

Step 6. If $(\hat{\gamma}_{1t} \in I_2$ and $\hat{\gamma}_{2t} \le UCL_2)$ or $(\hat{\gamma}_{1t} \in I_3$ and $\hat{\gamma}_{2t} \ge LCL_2)$, the process is considered to be IC, and returns to Step 1. Otherwise, the control flow proceeds to Step 7.

Step 7. The DS-γ chart detects an out-of-control at t^{th} sample number. Straightway actions are needed to diagnose the assignable cause(s).

Based on the procedure above, the properties of DS-γ chart are presented. Let Pa is the probability that the process is concluded to be statistically IC after conceiving both the information supplied by first and second samples [16]. Then Pa is defined as

$$P_a = P_{a1} + P_{a2} \tag{6}$$

where P_{a1} and P_{a2} are the probabilities of the process is concluded as IC in first and second sample stage, respectively. According to Step 3 and Step 6 in operational procedure of DS-γ chart, the probability P_{a1} and P_{a2} are derived as [18],

$$\begin{aligned} P_{a1} &= P(LWL \le \hat{\gamma}_{1t} \le UWL) = P(\hat{\gamma}_{1t} \le UWL) - P(\hat{\gamma}_{1t} \le LWL) \\ &= F_{\hat{\gamma}}(UWL \mid n_1, \gamma) - F_{\hat{\gamma}}(LWL \mid n_1, \gamma) \end{aligned} \tag{7}$$

$$\begin{aligned} P_{a2} &= P(UWL \le \hat{\gamma}_{1t} \le UCL_1 \text{ and } \hat{\gamma}_{2t} \le UCL_2) + P(LCL_1 \le \hat{\gamma}_{1t} \le LWL \text{ and } \hat{\gamma}_{2t} \ge LCL_2) \\ &= \left\{ \left[F_{\hat{\gamma}}(UCL_1 \mid n_1, \gamma) - F_{\hat{\gamma}}(UWL \mid n_1, \gamma) \right] \times F_{\hat{\gamma}}(UCL_2 \mid n_2, \gamma) \right\} + \\ &\quad \left\{ \left[F_{\hat{\gamma}}(LWL \mid n_1, \gamma) - F_{\hat{\gamma}}(LCL_1 \mid n_1, \gamma) \right] \times \left[1 - F_{\hat{\gamma}}(UCL_2 \mid n_2, \gamma) \right] \right\} \end{aligned} \tag{8}$$

where $F_{\hat{\gamma}}(x \mid n, \gamma)$ is defined in Eq. (4).

It can be seen here that based on Eq. (8), determining the process conditions in the second sample stage is only determined by second sample information. Whereas the DS concept should involve the first and second sample information in determining the process condition in second sample stage (see [16] and [20]). For this reason, the next section, a modified of the DS-γ chart is proposed, considering the combined information from the first and second samples to draw conclusions in the second sample stage.

3.2. Proposed of modified DS-γ chart (DS-G chart)

In this subsection, we presented a modified chart to enhance the DS-γ chart's performance for monitoring the CV, denoted DS-*G* chart. Referring to Fig. 1, define an additional interval, $I_5 = [LCL_2, UWL_2]$ (see Fig. 2) and replace the symbol $\hat{\gamma}$ by *G* to denote the sample CV for the DS-*G* chart. Then the modified operational procedure for this chart proposed as follow: We navigate the operational procedure of the previous DS-γ chart, except Step 5 and Step 6, where

Step 5a. If $G_{1t} \in I_2$ or $G_{1t} \in I_3$, take the second sample of size n_2, $X_{2i,t}$, $i = 1,2,...,n_2$, from the population of the first sample, then compute $\bar{X}_{2t}$ and S_{2t} using Eq. (2) and with $m = n_2$, as the sample mean and standard deviation of the second sample, respectively.

Step 5b. Compute the combine sample CV, $G_{2t} = S_{pt} / \bar{X}_{pt}$, at sample number *t*, where $\bar{X}_{pt}$ and S_{pt} are the combined sample mean and standard deviation which calculated by

$$\bar{X}_{pt} = \frac{n_1\bar{X}_{1t} + n_2\bar{X}_{2t}}{n_1 + n_2} \text{ and } S_{pt} = \left(\frac{(n_1-1)S_{1t}^2 + (n_2-1)S_{2t}^2}{n_1+n_2-2}\right)^{1/2}$$

Step 6. If $(G_{1t} \in I_2 \text{ or } G_{1t} \in I_3)$ and $G_{pt} \in I_5$, then the proses is considered as IC, and return to Step 1. Otherwise the process is considered as OC, and the control flow proceeds to Step 7.

Now, we present the properties of DS-*G* chart. Let P_a in Eq. (6) for the DS-*G* chart is denoted as P_a^*, then P_a^* is defined as

$$P_a^* = P_{a1}^* + P_{a2}^* \tag{9}$$

Based on the formulas in Eq. (5) and according to Step 3 and Step 6 in operational procedure of DS-*G* chart, the probability P_{a1}^* and P_{a2}^* are obtained as

$$P_{a1}^* = P_a \tag{10}$$

$$\begin{aligned} P_{a2}^* &= \left\{\left[P(UWL \le G_{1t} \le UCL_1 \text{ or } LCL_1 \le \hat{\gamma}_{1t} \le LWL)\right] \text{and } (LCL_2 \le G_{pt} \le UCL_2)\right\} \\ &= \left\{\left[F_{G_1}\left(UCL_1 \mid n_1,\gamma\right) - F_{G_1}\left(UWL \mid n_1,\gamma\right)\right] + \left[F_{G_1}\left(LWL \mid n_1,\gamma\right) - F_{G_1}\left(LCL_1 \mid n_1,\gamma\right)\right]\right\} \times \\ &\quad \left[F_{G_p}(LCL_2 \mid (n_1+\mathrm{n}_2),\gamma) - F_{G_p}(LCL_2 \mid (n_1+\mathrm{n}_2),\gamma)\right] \end{aligned} \tag{11}$$

where $F_{G_1}(x \mid n,\gamma)$ is defined from Eq. (4), while the c.d.f, $F_{G_p}(x \mid n_1+n_2,\gamma)$ of G_p in Eq. (11) will be determined based on the following proposition.

Proposition. Let $\boldsymbol{X_1} = \{X_{11}, X_{12}, ..., X_{1n_1}\}$ and $\boldsymbol{X_2} = \{X_{21}, X_{22}, ..., X_{2n_2}\}$ are the collection of random samples from a normal distribution with mean, μ, and variance, σ2. Let $\bar{X}_k$ and S_k^2, k = 1,2, are kth the sample mean and variance of $\boldsymbol{X_k}$, k = 1,2, respectively. Suppose $\bar{X}_p$ and S_p^2 are the mean and variance of the combine sample of $\boldsymbol{X_1}$ and $\boldsymbol{X_2}$ which are defined as

$$\bar{X}_p = \frac{n_1\bar{X}_1 + n_2\bar{X}_2}{n_1+n_2} \quad \textit{and} \quad S_p^2 = \frac{(n_1-1)S_1^2 + (n_2-1)S_2^2}{n_1+n_2-2},$$

respectively. Then

$$\frac{\left(\sqrt{n_1+n_2}\right)\bar{X}_p}{S_p} \sim T_{\upsilon,\delta}$$

where $T_{\upsilon,\delta}$ *follows a non-central t-distribution with* $\upsilon = n_1 + n_2 - 2$ *degree of freedom and non-centrality parameter* $\delta = \left(\sqrt{n_1+n_2}\right)\frac{\mu}{\sigma}$.

Proof. We know that $\bar{X}_k \sim \mathrm{N}(\mu,\sigma^2/n_k)$ and $\frac{(n_k-1)S_k^2}{\sigma^2} \sim \chi^2_{n_k-1}$, for k = 1,2, it follows that

$$Z = \frac{\left(\sqrt{n_1+n_2}\right)\left(\bar{X}_p-\mu\right)}{\sigma} \sim \mathrm{N}(0,1) \text{ and } W = \frac{(n_1+n_2-2)S_p^2}{\sigma^2} \sim \chi^2_{n_1+n_2-2}$$

We also know that $\bar{X}_k$ is independent of S_k^2, for k = 1,2. Because $\bar{X}_p$ is a function of $\left\{\bar{X}_1,\bar{X}_2\right\}$ and S_p^2 is a function of $\left\{S_1^2,S_2^2\right\}$, it follows that $\bar{X}_p$ is independent of S_p^2. Therefore,

$$\frac{\sqrt{n_1+n_2}\,\bar{X}_p}{S_p} = \frac{\left(\sqrt{n_1+n_2}\right)\left(\bar{X}_p-\mu\right)+\left(\sqrt{n_1+n_2}\right)\mu}{\sqrt{S_p^2}}$$

$$= \frac{\dfrac{\left(\sqrt{n_1+n_2}\right)\left(\bar{X}_p-\mu\right)}{\sigma}+\dfrac{\left(\sqrt{n_1+n_2}\right)\mu}{\sigma}}{\sqrt{\dfrac{(n_1+n_2-2)S_p^2}{(n_1+n_2-2)\sigma^2}}} = \frac{Z+\dfrac{\left(\sqrt{n_1+n_2}\right)\mu}{\sigma}}{\sqrt{\dfrac{W}{(n_1+n_2-2)}}} = \frac{Z+\delta}{\sqrt{\dfrac{W}{\upsilon}}} \sim T_{\upsilon,\delta}$$

Since $Z \sim \mathrm{N}(0,1)$ and $W \sim \chi^2_{n_1+n_2-2}$, then $T_{\upsilon,\delta}$ follows a non-central *t*-distribution with $\upsilon = n_1+n_2-2$ degree of freedom and non-centrality parameter $\delta = \left(\sqrt{n_1+n_2}\right)\mu/\sigma$.

According to Proposition above, since $G_p = S_p/\bar{X}_p$, then the c.d.f. of G_p can be approximated by

$$F_{G_p}\left(x \mid n_1+n_2,\gamma\right) = 1-F_T\left(\frac{\sqrt{n_1+n_2}}{x}\middle| n_1+n_2-2,\frac{\sqrt{n_1+n_2}}{\gamma}\right)$$

Since the IC process in CV is denoted as $\gamma=\gamma_0$, then the OC process in CV occurs when $\gamma=\gamma_1$, i.e. $\gamma_1=\tau\gamma_0$ for a specific shift $\tau\neq 1$, where τ represents the size of shift in a process CV. Note that the downward shift and upward shifts in CV are denoted as $\tau\in(0,1)$ and $\tau>1$, respectively.

3.3. Optimal design of DS-G chart

An optimal design of the DS-*G* chart is described in this subsection. As Ng et al [18], ANOS value is used to evaluate the performance of DS-*G* chart, so that can be compared with DS-γ chart. The ANOS is calculated as [21],

$$\mathrm{ANOS} = \frac{E[N]}{1-P_a^*} = \mathrm{ASS}\times\mathrm{ARL} \tag{12}$$

where

$$E[N] = n_1 + n_2 \times\left\{\left[F_{G_1}\left(UCL_1 \mid n_1,\gamma\right)-F_{G_1}\left(UWL \mid n_1,\gamma\right)\right]+\left[F_{G_1}\left(LWL \mid n_1,\gamma\right)-F_{G_1}\left(LCL_1 \mid n_1,\gamma\right)\right]\right\} \tag{13}$$

is the average sample size (ASS), and P_a^* is defined from Eq. (9). Note that the right hand side of Eq. (12), i.e. (ASS × ARL) is stated by the authors, therefore the ANOS formula has involved the ASS and the average run length (ARL) indicator for measuring the performance of control chart.

Let the ANOS value is notated as IC-ANOS (OC-ANOS) and the ASS is notated as IC-ASS (OC-ASS), when the process is IC (OC), respectively. Then the optimal design of DS-*G* chart is conducted by minimizing OC-ANOS which is mathematically expressed as follows

$$\min_{n_1,n_2,W,L_1,L_2} \text{OC-ANOS}(\tau), \tag{14}$$

subject to the constraints ANOS = IC-ANOS and IC-ASS = n, when the process is IC, i.e. when τ = 1. In the remaining sections of the paper, we assume that IC-ANOS = 200 and n = 5. Here, n is defined as the ASS when the process is IC.

4. Numerical analysis and comparison

In this section, numerical analysis is performed to acquire the optimal parameters of DS-G chart, using the methodology described in subsection 3.3 by minimizing OC-ANOS. Castagliola et al. [3] stated that the adaptive CV-type charts are not robust in observing the downward shifts, i.e. $\tau \in (0,1)$, thus this paper examines this chart's performance for upward shifts, i.e. $\tau \in \{1.1,\ 1.25,\ 1.5,\ 2.0\}$.

The optimal parameters (n_1, n_2, W, L_1, L_2) and the corresponding values of OC-ANOS for the DS-G chart, when the selected value of n = 5, $\gamma_0 \in \{0.1,\ 0.15,\ 0.2,\ 0.5\}$ and IC-ANOS = 200 are given in Table 1. The OC-ANOS(τ) values are computed by using Eq. (12) for selected value of $\tau \in \{1.1,\ 1.25,\ 1.5,\ 2.0\}$.

Table 1. The optimal parameters (n_1, n_2, W, L_1, L_2) corresponding to the OC-ANOS values for DS-*G* chart, when *n* = 5, $\gamma_0 \in \{0.1,\ 0.15,\ 0.2,\ 0.5\}$ and $\tau \in \{1.1,\ 1.25,\ 1.5,\ 2.0\}$ for IC-ANOS = 200.

τ	$\gamma_0 = 0.10$						$\gamma_0 = 0.15$					
	n_1	n_2	W	L_1	L_2	OC-ANOS	n_1	n_2	W	L_1	L_2	OC-ANOS
1.10	4	6	1.773	3.062	1.787	90.221	4	6	1.760	3.091	1.750	90.489
1.25	4	6	1.778	3.111	1.711	38.197	4	6	1.764	3.134	1.691	38.563
1.50	4	5	1.661	3.104	1.896	16.351	4	5	1.646	3.105	1.906	16.578
2.00	4	4	1.499	3.028	2.271	7.735	4	4	1.487	4.042	2.253	7.854
τ	$\gamma_0 = 0.2$						$\gamma0 = 0.5$					
	n_1	n_2	W	L_1	L_2	OC-ANOS	n_1	n_2	W	L_1	L_2	OC-ANOS
1.10	4	6	1.736	3.077	1.796	91.046	4	5	1.398	3.589	1.688	98.277
1.25	4	6	1.741	3.132	1.711	39.109	4	5	1.400	3.642	1.641	46.078
1.50	4	5	1.627	3.133	1.886	16.913	4	5	1.400	3.642	1.641	21.536
2.00	4	4	1.469	3.053	2.263	8.03	4	5	1.400	3.642	1.641	10.831

Table 2. A relative percentage of OC-ANOS improvement between the DS-*G* and DS-*γ* chart based on OC-ANOS of SH-*γ* chart, when *n* = 5, $\gamma_0 \in \{0.1,\ 0.15,\ 0.2,\ 0.5\}$ and $\tau \in \{1.1,\ 1.25,\ 1.5,\ 2.0\}$ for IC-ANOS = 200.

τ	$\gamma_0 = 0.1$		$\gamma_0 = 0.15$		$\gamma_0 = 0.2$		$\gamma_0 = 0.5$	
	DS-G	DS-γ	DS-G	DS-γ	DS-G	DS-γ	DS-G	DS-γ
1.10	26.56%	23.69%	26.70%	23.98%	26.76%	24.32%	27.27%	26.38%
1.25	31.21%	27.33%	31.42%	27.77%	31.67%	28.32%	34.79%	32.35%
1.50	26.69%	17.96%	27.09%	18.74%	27.60%	19.74%	32.99%	28.60%
2.00	19.84%	10.24%	20.38%	11.08%	21.06%	12.19%	25.74%	20.76%

Table 1 tells us that the sensitivity of the DS-*G* chart increases in detecting the shift by decreasing the OC-ANOS value when *τ* value increase. For example, by considering γ_0 = 0.1, the OC-ANOS = 38.197 for *τ* = 1.25 which is smaller than OC-ANOS = 90.221 for *τ* = 1.1. Additionally, from Table 1, for the upward shift (*τ* > 1), we need more observations to detect the smaller shift, i.e. the value of *τ* is closer to 1. Moreover, the OC-ANOS values increase, when γ_0 values increases. It means the sensitivity of DS-*G* chart is affected by changes in the value of γ_0, nevertheless the effect of γ_0 is small, especially for small γ_0.

For a comparison performance between the DS-*G* and DS-*γ* chart, we use the relative percentage of OC-ANOS improvement based on OC-ANOS of SH-*γ* chart, notated %OC-ANOS. Here, %OC-ANOS is defined as

$$\%\text{OC-ANOS}_w = \frac{\text{OC-ANOS}_{\text{SH-}\gamma} - \text{OC-ANOS}_{\text{DS-}w}}{\text{OC-ANOS}_{\text{SH-}\gamma}}$$

where $\text{OC-ANOS}_{\text{SH-}\gamma}$ is OC-ANOS of SH-*γ* chart and $\text{OC-ANOS}_{\text{DS-}w}$, $w \in \{G, \gamma\}$, are OC-ANOS of DS-*G* and DS-*γ* chart, respectively. Here, the value of $\text{OC-ANOS}_{\text{DS-}\gamma}$ is obtained by Ng et al [18]. It is noted that a control chart is accounted to perform better than the competitor if it has the larger %OC-ANOS, when IC-ANOS, *n*, and τ are fixed.

Table 2 shows the relative percentage of OC-ANOS improvement based on OC-ANOS of SH-γ chart. From Table 2, we can see that, $\text{\%OC-ANOS}_G$ is larger than $\text{\%OC-ANOS}_\gamma$ for all values of selected shifts τ and γ_0. This implies that the DS-*G* chart outperforms the DS-γ chart.

5. Conclusions

The numerical result has shown that the sensitivity of the DS-*G* chart increases in detecting the CV shifts by decreasing the OC-ANOS value when τ value increase. Additionally, for the upward shift ($\tau > 1$), we need more observations to detect the smaller shift. Furthermore, the comparison result showed that the DS-*G* chart outperform the DS-γ chart by giving larger values of relative percentage of OC-ANOS improvement.

References

[1] Reed G F, Lynn F and Meade B D 2002 *Clin. Diagn. Lab. Immunol.* **9** 1235–1239
[2] Gauri S K 2005 *Quality Engineering* **17** 633–640
[3] Castagliola P, Achouri A, Taleb H, Celano G and Psarakis S 2013 *Quality and Reliability Engineering International* **29** 1135–1149
[4] Zhang J, Li Z, Chen B and Wang Z 2014 *Computers & Industrial Engineering* **78** 205–212
[5] Zhang J, Li Z and Wang Z 2018 *Quality and Reliability Engineering International* **34** 188–202
[6] Mucha J and Witkowski W 2013 *Thin-Walled Structures* **66** 39–49
[7] Kang C W, Lee M S, Seong Y J and Hawkins D M 2007 *Journal of quality technology* **39** 151–158
[8] Hong E P, Kang C W, Baek J W and Kang H W 2008 Journal of the society of Korea Industrial and Systems Engineering **31**
[9] Castagliola P, Celano G and Psarakis S 2011 *Journal of Quality Technology* **43** 249–265
[10] Calzada M E and Scariano S M 2013 *Journal of Statistical Computation and Simulation* **83** 853–867
[11] Castagliola P, Achouri A, Taleb H, Celano G and Psarakis S 2015 *The International Journal of Advanced Manufacturing Technology* **80** 1561–1576
[12] Amdouni A, Castagliola P, Taleb H and Celano G 2015 *The International Journal of Advanced Manufacturing Technology* **81** 1–14
[13] Amdouni A, Castagliola P, Taleb H and Celano G 2017 *International Journal of Production Research* **55** 5521–5536
[14] Khaw K W, Khoo M B, Yeong W C and Wu Z 2017 *Communications in Statistics-Simulation and Computation* **46** 5772–5794
[15] Croasdale R 1974 *International Journal of Production Research* **12** 585–592
[16] Daudin J J 1992 *Journal of Quality Technology* **24** 78–87
[17] Irianto D and Shinozaki N 1998 *International Journal of Industrial Engineering-Applications and Practice* **5** 226–234
[18] Ng P S, Khoo M B C, Saha S and Yeong W C 2018 *2nd International Conference on Smart Sensors and Application (ICSSA) 2018* (IEEE) pp 93–98
[19] Iglewicz B, Myers R H and Howe R B 1968 *Biometrika* **55** 580–581
[20] He D and Grigoryan A 2002 *Quality and reliability engineering international* **18** 343–355
[21] Saha S, Khoo M B, Lee M H and Castagliola P 2018 *Communications in Statistics-Simulation and Computation* **47** 1353–1369